8.5 EVIDENCE OF NIGHTTIME WAVE-TURBULENCE INTERACTIONS ABOVE A HARDWOOD FOREST CANOPY

April L. Hiscox* and David R. Miller
University of Connecticut, Storrs, Connecticut

Carmen J. Nappo
NOAA, ARL, ATDD, Oak Ridge, Tennessee

1. INTRODUCTION

Lee et al. (1997) have shown that gravity waves can exist above a forest canopy. Presented here are the initial results of a preliminary study designed to investigate the effects of these waves on local atmospheric turbulence and smoke plume dispersion in the stable boundary layer. This study was designed to meet two objectives. The first was to determine if it is possible to estimate plume dispersion parameters from lidar images. The second was to explore if there is a relation between plume dispersion, wave motion, and turbulence above a forest canopy.

2. DESCRIPTION OF DATA SET

2.1 *Lidar Measurements*

The principles of lidar are similar to those of radar. The fundamentals can be found in Measures (1992) and Kovalev and Eichinger (2004). Specific details on The University of Connecticut miniature elastic lidar system can be found in Table 1. The system is capable of taking two different types of scans. The first, a 2D scan, creates a single slice of the plume by scanning through a series of elevations at a single azimuth to create a vertical scan, or scanning through a series of azimuths at a single elevation to create a horizontal scan. The second, a 3D scan, is a collection of 2D scans which produces a three-dimensional image of the plume from a series of either horizontal or vertical scans. For this study, a single 3D scan was completed in less than 2.5 minutes. Both 2D scans and 3D scans were taken to examine the plumes generated for this study.

The data presented here was taken on the night of October 7, 2003 at the University of Connecticut Research Farm in Coventry, Connecticut. A Rosco Laboratories, Inc. fog machine was used to create a tracer plume. Fog was released from a tower at a 35m height above the forest canopy (~23m). Plumes were advected mainly to the south of the release by a predominantly northerly wind. The tower was located at an azimuth of about 90° and a range of about 400m from the lidar.

Table 1: Lidar Hardware Configuration

Wavelength	1064nm
Energy per Pulse	125 mJ
Repetition Rate	50Hz
Pulse Width	< 15 ns
Pulse to pulse stability	±3%
Detector Type	Avalanche photodiode
High Quantum Efficiency	40%
Useful area	7 mm^2

2.2 *Micrometeorology Measurements*

A 3D sonic anemometer was located on the research tower at a height of 30 meters. Measurements of horizontal and vertical wind components as well as temperature were recorded at a rate of 20 Hz.

3. DATA ANALYSIS

3.1 *Dispersion parameters from repetitive 2D scans*

The 3D reference coordinate system for the lidar system is illustrated in Figure 1. In this system the lidar is located at the origin and the tracer release was located at (0,400m, 35m).

A set of 600 vertical 2D scans were taken at an azimuth of 96°, scanning in elevation from 2.5° to 6.5° with an increment of 0.1°. Each scan was completed in approximately 6 seconds. This method of data collection allowed for observation of the plume as it passed through a vertical plane.

* *Corresponding author address:* April L. Hiscox, UCONN, Department of Natural Resources Management and Engineering, 1376 Storrs Road, U-4087, Storrs, CT 06269-4087; e-mail: April.Hiscox@uconn.edu

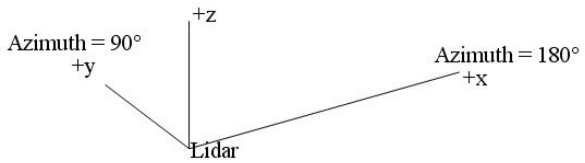

Figure 1: Coordinate system definition

All of the lidar data was preprocessed by background subtraction and range correction (Measures, 1992) and transformed into the correct coordinate system through the following equations,

$$x = range * \cos(elevation)\cos(azimuth) \quad (1)$$

$$y = range * \cos(elevation)\sin(azimuth) \quad (2)$$

$$z = range * \sin(elevation) \quad (3)$$

where the range is based on the location of the datapoint in the lidar array, the lidar resolution and the cosine of the elevation. The overall scanning range was 200 to 700 meters.

The total dispersion parameter (σ_T) is defined as the sum of the instantaneous dispersion parameter (σ_I) and the vertical plume meander (σ_m), i.e.

$$\sigma_T^2 = \sigma_i^2 + \sigma_M^2 . \quad (4)$$

The plume meander term, σ_m, represents the RMS value of the height of the maximum backscatter over the entire data collection period.

Using the lidar data, an instantaneous vertical dispersion parameter can be found for each 6-second slice based on an inversion of the Gaussian plume equation:

$$\sigma_i^2 = \frac{(\Delta z/2)^2}{-2\ln\alpha}, \quad (6)$$

where Δz is the vertical width of the plume, and α is a constant based on the ratio of the backscatter value at the edge of the plume to the maximum backscatter within the plume (see for exampled: Gifford, 1980). The instantaneous plume width is taken to be the vertical separation of a contour line with the same value for each plume. Figure 2 shows a typical plume slice, with the white line defining the plume edge as indicated above. Table 2 lists all of the relevant parameters for this slice. If a slice did not contain enough information to perform the calculations it was removed from this analysis. The two most prevalent reasons for removal were the plume moving above or below the region scanned, or the plume separated into more than one piece, making it impossible to identify a center point.

The above technique was used to create a one-hour time series of σ_i, Z_i, and Δz. A linear interpolation was used to establish values for the plumes that were eliminated. A 3-minute running mean was used to calculate values of turbulent kinetic energy (TKE) from the sonic anemometer data for the corresponding time period.

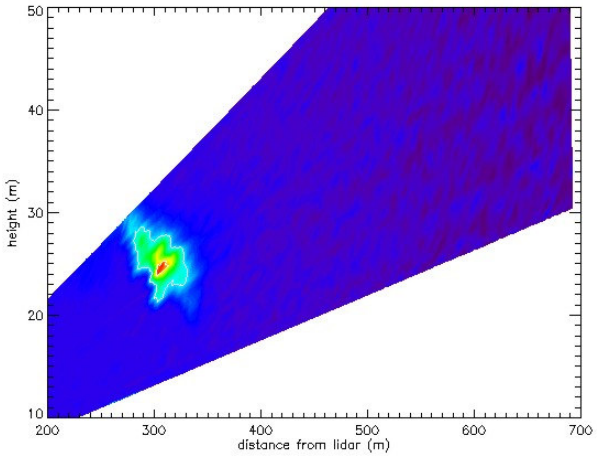

Figure 2: A representative single scan lidar slice. The contour colors represent relative backscatter intensities, with red being the strongest signal.

Table 2: Plume parameters for the slice shown in fig 2.

Z_{iE} (height of plume edge)	28.2 m
Z_i (height of plume center)	25 m
Y_c (range to plume center)	308 m
Δz (Plume width)	6.8 m
Maximum backscatter (relative units)	7.1e7
σ_i	1.3 m

4. RESULTS

Figure 3 presents the time series of vertical wind velocity, W, and plume height Z_i. It is expected that in the presence of a wave, the plume will rise and fall with the wave period. The mean plume height drops 5 meters over the course of the night. During the course of the experiment, the plume height rises and falls with a period of approximately 4 minutes. The vertical velocity appears to be quasi-periodic with the same 4-minute period, although many shorter variations are present. We consider these to be wave-like variations in both parameters.

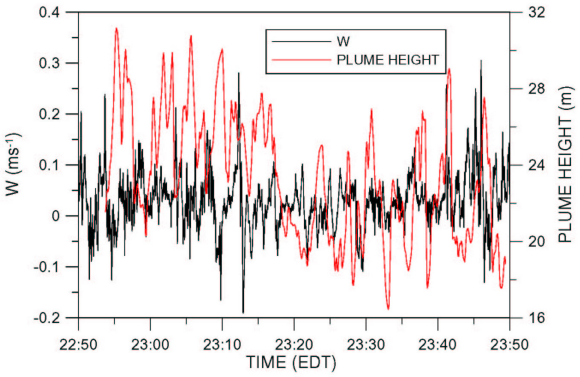

Figure 3: Time series of vertical wind velocity (W) and plume height (Z_i)

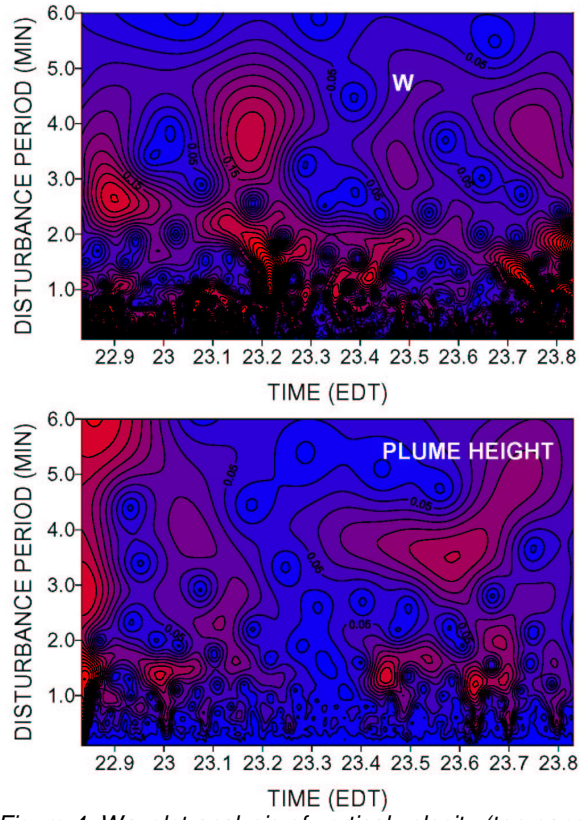

Figure 4: Wavelet analysis of vertical velocity (top panel) and plume height (bottom panel). Areas of red represent strong oscillations in the time series and areas of blue represent calmer periods

To further explore these variations, wavelet analysis of W and Z_i were performed and the results are presented in Figure 4. Both panels show many small variations with periods less than 2 minutes. The vertical wind velocity shows wavelike components with periods of 3 to 4 minutes as expected from the time series presented above. The plume height shows 3 to 4 minute oscillations early in the measurement period and then again between about 23.4 to 23.7h. The correspondence between these wavelet diagrams, although not strong, is taken as an indication of wave activity.

Figure 5 presents the time series of TKE and the σ_i. The TKE data shows a period of relative inactivity from about 23:15 EDT to 23:30 EDT. This same period of smaller magnitude and fewer fluctuations is seen in σ_i. It can also be seen that high frequency periods of TKE correspond to frequency periods of σ_i.

The wavelet analysis of TKE and σ_i is shown in Figure 6. The TKE shows a strong 4-minute wave structure at time 23.2, and strong 3-minute wave structure at the beginning of the measurement period, but no corresponding structure is seen in the σ_i wavelet. The period of relatively weak wave activity between 23.2h and 23.5h is the same low activity period seen in the time series of Figure 5.

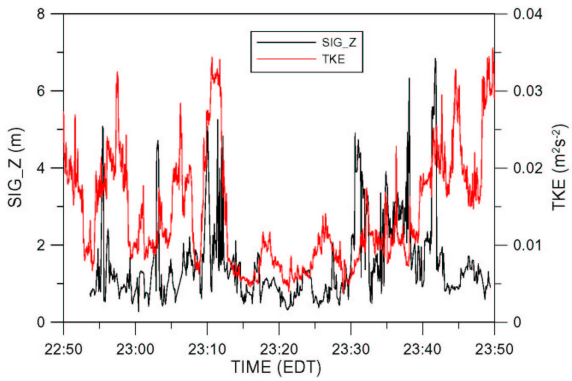

Figure 5: Time series of σ_i and 3 minute running average of TKE for the full hour of the experiment.

The TKE and σ_i wavelet results, do, however, show some correspondence in the higher frequencies, i.e., 23.1h and 23.7h. While it was expected that there would be more agreement than shown in this analysis, there are several reasons for this.

One such possibility is that we have used a technique to estimate σ_i from a Gaussian plume assumption, which should not necessarily apply to instantaneous plume slices. Another possible reason is the averaging period chosen for determining the TKE. Changes in the averaging interval could alter these results.

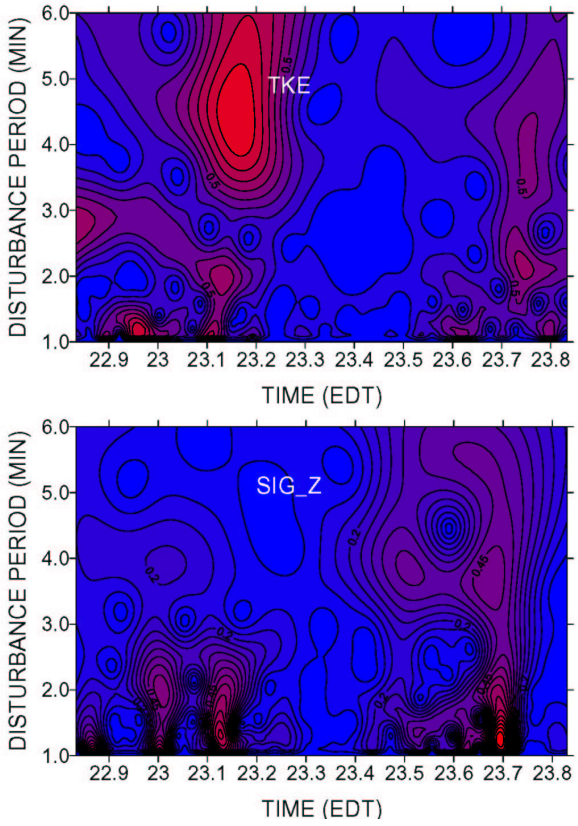

Figure 6: Wavelet analysis of TKE (top panel) and σ_z (bottom panel)

5. CONCLUSIONS

At this stage of research, two conclusions can be made. The first is that plume dispersion parameters can be inferred from lidar measurements. The second conclusion is that these parameters change with the local turbulence which suggests that wave-turbulence interactions may exist above a forest canopy.

7. ACKNOWLEGEMENTS

This work was performed under an informal agreement between the University of Connecticut Atmospheric Research Lab in the Department of Natural Resources Management and Engineering and the NOAA, ARL Atmospheric Turbulence and Diffusion.

The corresponding author would like to thank the UCONN College of Agricultural and the Department of Natural Resources Management and Engineering for providing financial support for this work through the departmental PhD assistantship program.

6. REFERENCES

Gifford, F.A., 1980: Smoke as a quantitative atmospheric diffusion tracer. *Atmospheric Environment*, **14**, 1119-1121.

Lee, X., H.H.Neumann, G. Den hartog, J. D. Fuenntes, T. A. Black, R. E. Mickle, P.C. Yang and P.D. Blanken, 1997: Observation of Gravity Waves in a Boreal Forest, *Boundary-Layer Meteorology*, **84**, 383-398.

Measures, R. M., 1992: *Laser Remote Sensing: Fundamentals and Applications*. Krieger Publishing Company, 510.

Kovalev, V.A. and W.E. Eichinger, 2004: *Elastic Lidar: Theory, Practice and Analysis Methods,* Wiley-Interscience, 615.